The assembly modes of rigid 11-bar linkages

Ioannis Z. Emiris, Guillaume Moroz

The assembly modes of rigid 11-bar linkages

Ioannis Z. Emiris*
National & Kapodistrian University of Athens
Greece

Guillaume Moroz†
INRIA Nancy
France

October 13, 2017

Abstract

Designing an m-bar linkage with a maximal number of assembly modes is important in robot kinematics, and has further applications in structural biology and computational geometry. A related question concerns the number of assembly modes of rigid mechanisms as a function of their nodes n, which is uniquely defined given m. Rigid 11-bar linkages, where $n = 7$, are the simplest planar linkages for which these questions were still open. It will be proven that the maximal number of assembly modes of such linkages is exactly 56.

The rigidity of a linkage is captured by a polynomial system derived from distance, or Cayley-Menger, matrices. The upper bound on the number of assembly modes is obtained as the mixed volume of a 5×5 system. An 11-bar linkage admitting 56 configurations is constructed using stochastic optimisation methods. This yields a general lower bound of $\Omega(2.3^n)$ on the number of assembly modes, slightly improving the current record of $\Omega(2.289^n)$, while the best known upper bound is roughly 4^n. Our methods are straightforward and have been implemented in Maple. They are described in general terms illustrating the fact that they can be readily extended to other planar or spatial linkages.

This version (2017) typesets correctly the last figure 5 so as to include all 28 configurations modulo reflection.

Keywords 11-bar linkage, assembly modes, polynomial system, mixed volume, distance matrix, cross entropy, simulated annealing

1 Introduction

Rigid mechanisms (or linkages) constitute an old but still very active area of research in mechanism and linkage theory, e.g. [Col02, FL95, WH07a, WH07b, Wun77] as well as computational geometry and structural bioinformatics, e.g. [BS04, EM99, JRKT01, Hav98, TD99].

A given linkage may be represented by a graph with edge set E of lengths $l_{ij} \in \mathbb{R}_+$, for $(i, j) \in E$. An assembly mode, or Euclidean embedding, in $\mathbb{R}^d$ is a mapping of its vertices to a set of points in $\mathbb{R}^d$, such that l_{ij} equals the Euclidean distance between the images of the i-th and j-th vertices, for $(i, j) \in E$. Euclidean embeddings impose no requirements on whether the edges cross each other or not. A linkage is (generically) *rigid* in $\mathbb{R}^d$ if and only if, for generic edge lengths it can be embedded in $\mathbb{R}^d$ in a finite number of ways, modulo rigid motions. A graph is *minimally rigid* if and only if it is no longer rigid once any edge is removed.

*emiris@di.uoa.gr
†guillaume.moroz@inria.fr

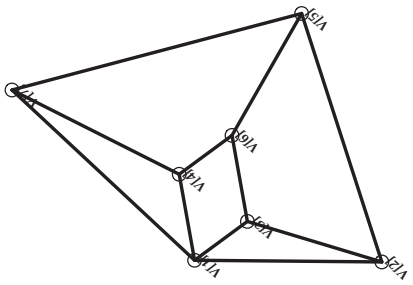

Figure 1: An 11-bar linkage.

Let us focus on planar linkages and the associated graphs. A graph is called *Laman* if and only if the number of edges is $2n-3$, where n is the number of vertices and, additionally, all of its vertex-induced subgraphs on $3 \leq k < n$ vertices have $\leq 2k-3$ edges. This is essentially the Grübler-Kutzbach-Chebychev formula on the degrees of freedom for mechanical linkages, e.g. [Ang89]. It is a fundamental theorem that the class of Laman graphs coincides with the generically minimally rigid planar linkages [Lam70]. The problem studied in this paper is to compute the number of distinct planar assembly modes of rigid mechanisms, up to rigid motions. In particular, the maximal number of assembly modes of an 11-bar linkage (Figure 1) will be presented for the first time.

1.1 Existing work

The algebraic approach is to define a well-constrained polynomial system expressing the length constraints, such that the system's real solutions correspond precisely to the different assembly modes. When defining a straightforward system such as (1), where the unknowns are the nodes' coordinates, all nontrivial equations are quadratic. For planar linkages, there are $2n-4$ equations hence, by applying the classical Bézout bound on the number of common roots, we obtain 4^{n-2}. It is indicative of the hardness of the problem that efforts to substantially improve these bounds have failed.

Today, the best general upper bound is roughly $4^{n-2}/\sqrt{\pi(n-2)}$. This was obtained using determinantal varieties defined by distance matrices [BS04]. Straightforward application of mixed volumes (discussed in Section 3) yields an upper bound of 4^{n-2} [ST10].

The best general lower bounds are $24^{\lfloor (n-2)/4 \rfloor} \simeq 2.21^n$ and $2 \cdot 12^{\lfloor (n-3)/3 \rfloor} \simeq 2.289^n/6$, obtained by a caterpillar and a fan [1] construction, respectively [BS04]. Both bounds are based on the Desargues graph (Figure 2), which admits 24 assembly modes.

In applications, it is crucial to know the number of assembly modes for specific (small) values of n. The most important result in this direction was to show that the Desargues linkage, also known as the planar parallel robot, admits precisely 24 assembly modes in the plane [BS04, Hun83, GSR92, LM94]. Moreover, the $K_{3,3}$, or 9-bar, linkage admits exactly 16 assembly modes in the plane [WH07a]. This paper demonstrated such a linkage through an elaborate construction which was not required in our case.

All existing bounds for $n \leq 10$ are found in Table 1 from [ETV09] [2].

[1] This slightly corrects the exponent of the original statement.

[2] see [ETV13] for an update.

$n=$	3	4	5	6	7	8	9	10
upper	2	4	8	24	64	128	512	2048
lower	2	4	8	24	48	96	288	576

Table 1: Bounds for the number of embeddings of rigid graphs with $n \leq 10$ [ETV09].

1.2 Our contribution

To upper bound the number of planar rigid mechanisms, we explore adequate polynomial systems leading to tight root bounds. Modeling physical systems by appropriate polynomial systems is a deep and hard question, with a wide range of applications in different fields.

We employ two powerful algebraic tools for defining polynomial systems and for counting the system's common roots. For the former, we use distance matrices, also known as Cayley-Menger matrices, which contain all known and unknown distances between the graph's nodes. The signs of the matrix minors capture rigidity and embeddability in Euclidean spaces, as described in Section 3. Our results indicate that such matrices are advantageous to using the coordinates' formulation, such as system (1), when constructing the polynomial system.

Our second tool is the mixed volume of a well-constrained polynomial system, which exploits the sparseness of the equations. The mixed volume bounds the number of common roots, by Bernstein's Theorem 1, as described in Section 3. This bound is never larger than Bézout's, and is typically much tighter for systems whose equations do not contain all possible terms for a given total degree. It turns out that such are the systems encountered here and could be of wider interest in similar enumeration problems.

Moreover, mixed volume is a bound so it only needs to consider which are the nonzero coefficients, without considering specific values. This is in sharp contrast to solving methods often used for root counting, where one assigns random values to the coefficients.

We thus obtain a tight bound for linkages with $n = 7$ nodes by appropriately formulating the polynomial system based on distance matrices. We compute the mixed volume of a 5×5 polynomial system, which equals 56. This is tight since we demonstrate a construction with as many assembly modes, see Figure 5. We also show how our stochastic optimisation methods are generalizable for studying further planar or spatial linkages. Our construction also yields a general lower bound of $\Omega(2.3^n)$ on the number of configurations, thus improving the available bound of $\Omega(2.289^n)$, whereas the best available upper bound is $O(4^n/\sqrt{n})$.

The rest of the paper is structured as follows. Section 2 presents rigid mechanisms and how our study focuses on a specific 11-bar linkage. Section 3 presents our algebraic tools and obtains the upper bound of 56 for 7 nodes and 11 bars. Section 4 actually constructs a linkage with 56 assembly modes. We conclude with open questions.

2 Rigid linkages

This section studies the number of assembly modes of planar rigid linkages or, equivalently, rigid graphs and their number of embeddings in $\mathbb{R}^2$.

Such linkages admit inductive constructions that begin with a triangle, followed by a sequence of so-called Henneberg steps. There are two types of such steps, each adding one new vertex and increasing the total number of edges by 2. A graph is Laman, or the associated mechanism is rigid, if and only if it can be constructed by a sequence of the corresponding Henneberg steps. By exploiting

this fact, all rigid graphs in $\mathbb{R}^2$, but also in $\mathbb{R}^3$, were constructed using the Henneberg steps in [ETV09], and classified up to graph isomorhism.

Let us consider the Henneberg steps defining Laman graphs, each adding a new vertex and a total number of two edges. A Henneberg-1 (or H_1) step connects the new vertex to two existing vertices. A Hennenerg-2 (or H_2) step connects the new vertex to 3 existing vertices having at least one edge among them, and this edge is removed. Both steps are illustrated in Figure 3. We represent each Laman graph by $\triangle s_4 \ldots, s_n$, where $s_i \in \{1, 2\}$; this is known as its Henneberg sequence. Note that this sequence is by no means unique. A Laman graph is called H_1 if and only if it can be constructed using only H_1 steps; it is called H_2 otherwise.

Since two circles intersect generically in two points, a H_1 step at most doubles the number of assembly modes and this is tight, generically. In Table 1 most lower bounds follow from this fact. The lower bound for $n = 9$ follows from the Desargues fan [BS04].

For a Laman graph on 6 vertices, a tight uppper bound of 24 follows by examining the only three possibilities: the graph is either H_1, it is $K_{3,3}$, or is the Desargues graph. Now, H_1 graphs on 6 vertices have exactly 16 assembly modes. The $K_{3,3}$ graph has precisely 16 assembly modes [WH07a], a fact first conjectured in [Wun77]. The Desargues graph has precisely 24 assembly modes: the upper bound was first shown in [Hun83] and proven more explicitly, along with the lower bound, in [GSR92]. This fact was independently rediscovered in [BS04] and proven via coupler curves.

In [ETV09] further upper bounds were obtained from the following family of simple systems, employed in order to express graph embeddability in $\mathbb{R}^2$. Let x_i, y_i denote the coordinates of the i-th vertex, where the l_{ij} are the given lengths:

$$\begin{cases} x_i = a_i,\ y_i = b_i, & i = 1, 2, \quad a_i, b_i \in \mathbb{R}, \\ (x_i - x_j)^2 + (y_i - y_j)^2 = l_{ij}^2, & (i, j) \in E - \{(1, 2)\} \end{cases} \tag{1}$$

Vertex (x_1, y_1) was fixed to $(0, 0)$, to discard translations, and (x_2, y_2) to $(1, 0)$ to remove rotations and scaling, assuming without loss of generality that the corresponding edge exists. Then the mixed volume of the system gave the upper bounds in the table which, unfortunately, are loose, even after removing roots at infinity [ETV09]. Below we overcome this limitation by considering polynomial systems derived from distance matrices.

We now study the case $n = 7$. If a H_1 step is applied to any linkage with $n = 6$, the resulting linkage with $n = 7$ admits exactly 48 assembly modes, which is reflected to the corresponding lower bound in Table 1. To maximize the number of assembly modes, we shall apply a H_2 step to any graph with $n = 6$. By checking graph isomorphisms and taking into account the various symmetries, it was shown [ETV09] that there are only 3 relevant graphs to be considered. These are obtained by a H_2 step applied to the Desargues graph as follows, where notation refers to Figure 2:
We remove edge $(4, 5)$, and add edges $(4, 7), (5, 7)$, and

- $(1, 7)$, or
- $(3, 7)$, or
- $(6, 7)$.

The first case corresponds to the topology that shall be studied extensively in the sequel, since it leads to the maximum number of 56 assembly modes. The linkage is shown in Figure ref11barLinkage and in the next section we will proove that 56 is the maximum number of assembly modes possible for such a linkage. The other two linkages admit at most 44 and 48 assembly modes, respectively, hence they are not studied any further. These upper bounds are obtained as mixed volumes of polynomial systems, as explained in Section 3.

3 Algebraic methods for the upper bound

This section discusses polynomial systems, describes distance matrices, and derives an upper bound on the number of assembly modes.

3.1 Mixed volume

We first discuss multivariate polynomial systems and introduce sparse elimination theory in order to exploit their structure and sparseness; for details, see [CLO05, Emi94]. Classical elimination theory characterizes every polynomial by its total degree. For a well-constrained system of polynomial equations, the classical Bézout bound on the number of isolated roots equals the product of the polynomials' total degrees. One disadvantage of this bound is that it counts projective roots and hence increases when there are roots at projective infinity.

In sparse (or toric) elimination theory, a polynomial is characterized by its support. Given a polynomial f in n variables, its support is the set of exponents in $\mathbb{N}^n$ corresponding to nonzero terms (or monomials). The Newton polytope of f is the convex hull of its support and lies in $\mathbb{R}^n$. Consider (Newton) polytopes $P_i \subset \mathbb{R}^n$ and parameters $\lambda_i \in \mathbb{R}, \lambda_i \geq 0$, for $i = 1, \ldots, n$. We denote by $\lambda_i P_i$ the corresponding scalar multiple of P_i. Consider the Minkowski sum of the scaled polytopes $\lambda_1 P_1 + \cdots + \lambda_n P_n \in \mathbb{R}^n$; its Euclidean volume is a homogeneous polynomial of degree n in the λ_i. The coefficient of $\lambda_1 \cdots \lambda_n$ is the *mixed volume* of $P_1, \ldots, P_n$. If $P_1 = \cdots = P_n$, then the mixed volume is $n!$ times the Euclidean volume of P_1.

We now focus on the topological torus $\mathbb{C}^* = \mathbb{C} - \{0\}$ in order to state Bernstein's root bound in terms of mixed volume.

Theorem 1 [Ber75] *Let $f_1 = \cdots = f_n = 0$ be a polynomial system in n variables with real coefficients, where the f_i have fixed supports.*

The number of isolated common solutions in $(\mathbb{C}^*)^n$ is bounded above by the mixed volume of the Newton polytopes of the f_i. This bound is tight for a generic choice of coefficients of the f_i's.

One alternative to using general bounds such as mixed volume is to manipulate a system, with coefficients chosen randomly, so as to bound the number of common real roots, e.g. by means of Gröbner bases or homotopy continuation. We actually used Gröbner bases for all systems studied in this paper, where we have used random coefficients. In particular, for the linkage analyzed below, we computed the total-degree Gröbner basis of system (1) with random distances in Maple, and obtained the Hilbert polynomial of the corresponding ideal.

This is a univariate polynomial where, by setting its variable to 1, one deduces an upper bound on the number of complex common roots. This was indeed 56, which coincides with mixed volume. However, this only offers an indication on the number of roots, not an actual bound, since it depends on the choice of coefficients.

The advantage of mixed volume is that it treats entire classes of systems defined by their nonzero terms, without considering specific coefficient values. Lastly, a tight mixed volume implies that one can solve the system efficiently either by sparse resultants, e.g. [CE00], or by sparse homotopies, e.g. [Ver99].

3.2 Distance geometry

The theory of distance geometry has been well developed, e.g. [Blu70, Sch35], with several applications especially in structural bioinformatics, e.g. [EM99, Hav98].

Definition 1 *Given an n-vertex graph, the corresponding* distance *or* Cayley-Menger matrix *is a symmetric* $(n+1) \times (n+1)$ *matrix* B*, indexed by* $i = 0, \ldots, n$*, such that* $B(0,i) = 1$ *for* $i \geq 1$*,* $B(i,i) = 0$ *for* $i \geq 0$*, and* $B(i,j)$ *equals the squared distance between vertices* i, j*, for* $j > i \geq 1$*.*

To be more precise, to obtain the Cayley-Menger matrix of the given n vertices, we must multiply B by $-1/2$. But for testing embeddability, the two formulations are equivalent, as seen in the following theorem, due to the work of Cayley and Menger, see [Blu70, Sch35]. Let $D(i_1, \ldots, i_k)$ denote the $(k+1) \times (k+1)$ diagonal minor of B indexed by rows and columns $0, i_1, \ldots, i_k$, where $i_1 < \cdots < i_k \in \{1, \ldots, n\}$.

Theorem 2 *Suppose we are given a matrix* B *of the form specified in Definition 1. Then* B *corresponds to a (complete) graph embeddable in* $\mathbb{R}^d$*, if and only if*

1. *for* $k = 2, \ldots, d+1$ *and any* $\{i_1, \ldots, i_k\} \subset \{1, \ldots, n\}$*, it holds* $(-1)^k D(i_1, \ldots, i_k) \geq 0$*, and*
2. *rank*$(B) = d + 2$*.*

The second condition, due to Cayley, yields a (large) number of equalities, which are typically not independent.

The first condition, due to Menger, yields inequalities: For $k = 2$, it expresses the fact that all entries must be non-negative. For $k = 3$, it captures the triangular inequality. If we apply it, without loss of generality, to indices $1, 2, 3$, using $c_{ij} = l_{ij}^2$ for the given entries, then the condition states that $D(1,2,3) \leq 0$, where this quantity equals

$$-(l_{12} + l_{13} + l_{23})(l_{12} + l_{13} - l_{23})(l_{12} + l_{23} - l_{13})(l_{13} + l_{23} - l_{12}).$$

This vanishes precisely when the corresponding points are collinear, whereas $D(1,2,3) < 0$ when the points define a triangle. Equivalently, $D(i,j,k) \leq 0$ can be written $l_{ik} + l_{jk} \geq l_{ij}$ for all triplets $i, j, k \in \{1, \ldots, n\}$. For $k = 4$ the condition captures the tetrangular inequality.

3.3 Upper bound

We shall employ the rank condition in order to derive equality constraints on the unspecified distances of our linkage. Here is the matrix, where the $c_{ij} = l_{ij}^2$ correspond to the fixed distances, and x_{ij} are the unspecified distances.

$$\begin{array}{c} \\ \\ v_1 \\ v_2 \\ v_3 \\ v_4 \\ v_5 \\ v_6 \\ v_7 \end{array} \begin{array}{c} \begin{array}{ccccccc} v_1 & v_2 & v_3 & v_4 & v_5 & v_6 & v_7 \end{array} \\ \left[\begin{array}{ccccccc} 0 & 1 & 1 & 1 & 1 & 1 & 1 & 1 \\ 1 & 0 & c_{12} & c_{13} & c_{14} & x_{15} & x_{16} & c_{17} \\ 1 & c_{12} & 0 & c_{23} & x_{24} & c_{25} & x_{26} & x_{27} \\ 1 & c_{13} & c_{23} & 0 & x_{34} & x_{35} & c_{36} & x_{37} \\ 1 & c_{14} & x_{24} & x_{34} & 0 & x_{45} & c_{46} & c_{47} \\ 1 & x_{15} & c_{25} & x_{35} & x_{45} & 0 & c_{56} & c_{57} \\ 1 & x_{16} & x_{26} & c_{36} & c_{46} & c_{56} & 0 & x_{67} \\ 1 & c_{17} & x_{27} & x_{37} & c_{47} & c_{57} & x_{67} & 0 \end{array}\right] \end{array}$$

By Theorem 2, any 5×5 minor of this matrix must vanish, which yields polynomial equations on the variables x_{ij}. There are $\binom{7}{3} = 35$ such minors, each in 2 to 4 variables. Among these polynomials, no 4×4 subsystem exists that corresponds to a rigid mechanism, as can be verified by checking Laman's condition. This is indispensable for the system to have a finite number of solutions.

However, it is possible to find certain 5×5 subsystems whose subgraph is Laman and, moreover, uniquely define the configuration of the overall linkage (Figure 4). One of these systems has 4 bivariate equations and one trivariate equation, and is defined by taking the following diagonal minors:

$$\begin{cases} D(4,5,6,7)(c_{46}, c_{47}, c_{56}, c_{57}, x_{45}, x_{67}) = 0 \\ D(1,4,6,7)(c_{14}, c_{17}, c_{46}, c_{47}, x_{16}, x_{67}) = 0 \\ D(1,4,5,7)(c_{14}, c_{17}, c_{47}, c_{57}, x_{15}, x_{45}) = 0 \\ D(1,2,3,5)(c_{12}, c_{13}, c_{25}, c_{23}, x_{15}, x_{35}) = 0 \\ D(1,3,5,6)(c_{13}, c_{36}, c_{56}, x_{15}, x_{16}, x_{35}) = 0 \end{cases} \tag{2}$$

defines a system of 3 quadratic and two cubic equations in $x_{15}, x_{16}, x_{35}, x_{45}, x_{67}$; the cubics are the first and last polynomials. Now, this system's mixed volume turns out to be 56, computed using the software from [EC95] [3]. This bounds the number of (complex) common system's solutions, hence the number of (real) assembly modes.

Notice that this bound does not take into account solutions with zero coordinates, in other words some zero length. However, a linkage has assembly modes with some zero length only when the input bar lengths form a singular set, in the sense that they would satisfy a non-generic algebraic dependency. For example, by letting some input distance be exactly 0, some 11-bar linkage may theoretically have infinitely many configurations. However, generically, it is impossible to have such a linkage.

Thus, the mixed volume bound guarantees that a true 11-bar linkage can have at most 56 assembly modes.

4 Lower bound

To prove that 56 is a lower bound on the number of configurations, it is sufficient to exhibit a linkage with 56 configurations. Unfortunately, we have 11 design parameters. Thus our search space is homeomorphic to $\mathbb{R}_+^{11}$. Even if we reduce the search space to the integers between 1 and 100 for each parameter, an exhaustive search would lead us to consider 10^{22} linkages.

Another approach was used in [LM94] to find a planar parallel robot with 12 real solutions. The authors found a singular positions with many real solutions, and use deformations to get the desired result. The advantage of this approach is that the space of singular configurations has a lower dimension than the full design space. However, in our case, the dimension was still too high and this approach could not allow us to conclude.

4.1 Stochastic methods

Random sampling is a common approach to search in high dimensional space is random sampling. The system at hand being homogeneous, we can specify the last coordinate l_{10} to 100 without restriction of generality. Moreover, in the following, we restrict our domain to integer coordinates.

Our goal is to maximize the function:

$$\begin{aligned} N : \quad & \mathbb{N}^{10} \to \mathbb{N} \\ & (l_0, ..., l_9) \mapsto \begin{cases} 0, \text{ if system (2) has infinitely many solutions.} \\ \text{Number of solutions of system (2), otherwise.} \end{cases} \end{aligned}$$

A first idea is to sample random points using a Gaussian law centered on an arbitrary initial point. This naive approach did not allow us to find a linkage with 56 configurations, but we could finally find such a point by using more sophisticated methods.

[3] http://www.di.uoa.gr/∼emiris/

4.1.1 Evaluation of the objective function

The cost of evaluating the objective function is the bottleneck of the stochastic methods. The function N needs to be evaluated several hundreds of time before converging toward a point where it is maximal.

In our case, evaluating N means solving a system of polynomial equations with finitely many solutions, and counting the number of its real positive roots. Experimentally, we use the Maple function `RootFinding[Isolate]`. This function computes isolating boxes around the real solutions of the system to solve. The underlying algorithm uses Grbner bases and Rational Univariate Representation.

The choice of the system modeling the 11-bar manipulator is critical. A naive modelling yields a system with 14 variables, one for each of the coordinates of the 7 vertices, and 11 equations, one for each link in the manipulator. In Maple, solving this system is roughly 10 times slower than solving System (2). That can be explained partly by the fact that, generically, the time complexity to solve a 0-dimensional system is roughly exponential in the number of variables, e.g. [CLO05, Laz01].

4.1.2 Simulated annealing

The Monte-Carlo simulation and its simulated annealing variant [KGJV83] are the most well spread stochastic optimisation methods. These methods have already been used in robotics for path planning in [KSLO96]. The convergence of these methods has been well studied and the simulated annealing simulations has been successfully used in different field such as biology and chemistry. We implemented this method to maximize the function N.

The Monte-Carlo simulation depends on a parameter T called temperature. In the simulated annealing variant, the temperature T is decreased according to a specific schedule at each step. The optimal way to decrease the temperature depends on each problem. In our case, we chose arbitrarily a linear cooling schedule ([SH87, NA98]). The corresponding pseudo-code is summarized in Algorithm 1.

4.1.3 Cross entropy method

A new method was introduced recently by Rubinstein in [Rub97] for the simulation of rare events. This method is especially well-suited for combinatorial and continuous optimization ([Rub99]). The idea of this approach consists in minimizing the distance between specific probability laws appearing during the computation (see [DBKMR05] for more details). For our problem, we use the scheme developed for continuous multi-extremal function optimization presented in [KPR06]. The function N is not continuous, but behaves smoothly: generically, if we modify the lengths of a given linkage by small enough values, the number of configurations is increased or decreased only by 2. For our problem it yields Algorithm 2.

4.2 Results

In Table 2, we compare the results of three stochastic methods used to optimize the function N with respect to the lengths of the 11-bar linkage.

The first column shows the result of the direct random sampling. Each line correspond to 600 evaluation of N on points chosen according to a Gaussian law of center 100 and standard deviation 100. This operation has been run 10 times, yielding a total of 6000 evaluations of N on random points. However, this did not allow us to find a linkage with 56 configurations.

The second approach is a Simulated Annealing simulation. We ran it 10 times, limiting the number of evaluations of N to 600. One of our simulation returned a set of link lengths yielding a linkage with 56.

Finally, the last column reports the results of the Cross Entropy Method. Each line correspond to a simulation stopped after 600 evaluations of N. This approach was the most efficient. Four simulations out of ten returned a linkage with 56 configurations.

The results of our stochastic methods are summarized in Table 2. In particular, we found that the manipulator with the following design parameters

$$\begin{array}{llll} l_0 = 180 & l_1 = 70 & l_2 = 200 & l_3 = 205 \\ l_4 = 210 & l_5 = 205 & l_6 = 80 & l_7 = 200 \\ l_8 = 70 & l_9 = 200 & l_{10} = 100 & \end{array}$$

has exactly 56 assembly modes. Some of its assembly modes are shown in Figure 5.

Our simulations show that the set of 11-bar linkages with 56 assembly modes has a non-zero volume. With the direct random sampling, we did not find any linkage with more than 48 assembly modes. This indicates that linkages with bar lengths between 0 and 300 have a very small probability to have 56 assembly modes. Our experiments show that the Cross Entropy method is a general approach well suited to generate such configurations. Moreover, it can be used easily for other mechanisms, such as larger planar or spatial linkages for example. A variant of this method can also be used to compute an estimation of the probability to find a linkage with a maximal number of assembly mode.

Direct Sampling	Simulated Anealing	Cross Entropy
44 (572)	52 (17)	52 (199)
42 (196)	54 (247)	54 (132)
48 (27)	48 (362)	52 (186)
44 (200)	52 (14)	54 (130)
42 (200)	54 (547)	56 (497)
44 (424)	54 (315)	**56** (328)
46 (48)	**56** (425)	**56** (454)
42 (170)	50 (585)	54 (375)
42 (18)	54 (26)	**56** (552)
46 (366)	52 (474)	**56** (355)

Table 2: Results of different stochastic optimisation algorithms. Each line corresponds to a simulation stopped after 600 evaluations of N. The results is of the form $n(m)$ where n is the maximal reached value of N and m is the number of evaluations done before reaching it.

5 Improvement on the general lower bound

This specific linkage allows us to improve slightly the lower bound on the maximal number of assembly modes of a planar linkage with n pivot joints. We use the same fan construction as in [BS04].

We construct a linkage with n nodes composed of k sub-mechanisms as follows. Each of the k sub-mechanisms is a 11-bar linkage with the topology we have considered so it has 56 assembly modes, and 28 when one triangle is fixed. All sub-mechanisms share this triangle so there are no degrees of freedom other than those within each sub-mechanism, and the overall mechanism is rigid. The total number of assembly modes equals the product of remaining assembly modes per sub-mechanism, since these sub-mechanisms can be configured independently. Hence the overall number is 28^k when one triangle is specified, and $2 \cdot 28^k$ in total. For n pivot joints, we let k be the greatest integer $\leq \frac{n-3}{4}$.

Algorithm 1 Simulated annealing with linear cooling to maximize the number of solutions of System (2)

$T_0 \leftarrow 4$
$maxStep \leftarrow 1000$
$\vec{\sigma} \leftarrow [10, ..., 10]$
$point \leftarrow \{l_0 = 100, ..., l_9 = 100\}$
$value \leftarrow N(l_0, ..., l_9)$
for n from 1 to $maxStep$ while $value < 56$ **do**

$newPoint \leftarrow GaussianNeighbour(point, \vec{\sigma})$
$newValue \leftarrow N(l_0, ..., l_9)$
$treshold \leftarrow$ Uniform random value in [0,1]
if $\begin{cases} newValue > value \\ \qquad or \qquad \text{then} \\ treshold < e^{\frac{newValue - value}{T}} \end{cases}$
$point \leftarrow newPoint$
$value \leftarrow newValue$
end if
$T \leftarrow T_0(1 - n/maxStep)$
end for
return point

This yields the lower bound:

$$2 \cdot 28^{\lfloor \frac{n-3}{4} \rfloor}$$

The constant under the exponent is $\sqrt[4]{28} \simeq 2.3003$ while in the previous lower bound the constant was $\sqrt[3]{12} \simeq 2.2894$.

6 Further work

Undoubtedly, the most important and oldest problem in rigidity theory is the full combinatorial characterization of rigid graphs in $\mathbb{R}^3$. We believe that one can extend our methods to spatial linkages. We expect our approach leads to an algorithmic process for obtaining good algebraic representations of the enumeration problem at hand, namely low mixed volumes for the systems derived from distance matrices. One issue is that the number of equations produced is quite large, with algebraic dependancies among them. The question becomes then to choose the best well-constrained system.

The structures studied in this paper are point-and-bar structures; they generalize to body-and-bar, where edges can be connected to different points of a rigid body. It is known that a body-and-bar structure in $\mathbb{R}^d$ is rigid if and only if the associated graph is the edge-disjoint union of $\binom{d+1}{2}$ spanning trees [WT85]. Body-and-bar structures are our next object of study.

Acknowledgements. I.Z. Emiris is partially supported by FP7 contract PITN-GA-2008-214584 SAGA: Shapes, Algebra, and Geometry. He also acknowledges fruitful discussions with Elias Tsigaridas. Both authors were inspired to work on this problem at the Workshop on Discrete and Algebraic Geometry in September 2010, at Val d'Ajol, France.

Algorithm 2 Cross Entropy Method to maximize the number of solutions of System (2)

$maxStep \leftarrow 600$
$N_{elite} \leftarrow 5$
$N \leftarrow 20$
$\alpha \leftarrow 0.5$
$\vec{\mu} \leftarrow [100, ..., 100]$
$\vec{\sigma} \leftarrow [100, ..., 100]$
$\gamma \leftarrow 0$
$max \leftarrow 0$
for n from 1 to $maxStep$ while $max < 56$ **do**
  for i from 1 to N **do**
    $\mathbf{X_i} \leftarrow GaussianNeighbour(\vec{\mu}, \vec{sigma})$
  end for
  $prevmax \leftarrow max$
  for i from 1 to N **do**
    $\mathbf{V}_i \leftarrow N(\mathbf{X_i})$
    if $\mathbf{V_i} > max$ **then**
      $max \leftarrow \mathbf{V}_i$
      $point \leftarrow \mathbf{X_i}$
    end if
  end for;
  Sort $\mathbf{X}$ and $\mathbf{V}$ from the largest $\mathbf{V}_i$ to the smallest
  $\gamma \leftarrow \mathbf{V}_{N_{elite}}$
  $\vec{\mu}^{new} \leftarrow \frac{1}{N_{elite}} \sum_1^{N_{elite}} \mathbf{X_i}$
  $\vec{\sigma}^{new} \leftarrow \sqrt{\frac{1}{N_{elite}} \sum_1^{N_{elite}} (\mathbf{X_i} - \vec{\mu}_i)^2}$
  $\vec{\mu} \leftarrow \alpha \vec{\mu}^{new} + (1 - \alpha)\vec{\mu}$
  $\vec{\sigma} \leftarrow \alpha \vec{\sigma}^{new} + (1 - \alpha)\vec{\sigma}$
end for
return point

References

[Ang89] J. Angeles. *Rational Kinematics*. Springer-Verlag, New York, 1989.

[Ber75] D.N. Bernstein. The number of roots of a system of equations. *Funct. Anal. and Appl.*, 9(2):183–185, 1975.

[Blu70] L.M. Blumenthal. *Theory and Applications of Distance Geometry*, volume 15. Chelsea Publishing Company, Bronx, NY, 2nd edition, 1970. (1st edition: Cambridge Univ. Press, Cambridge, 1953).

[BS04] C. Borcea and I. Streinu. The number of embeddings of minimally rigid graphs. *Discrete Comp. Geometry*, 31(2):287–303, 2004.

[CE00] J.F. Canny and I.Z. Emiris, A Subdivision-Based Algorithm for the Sparse Resultant, *J. ACM*, 47(3):417–451, 2000.

[CLO05] D. Cox, J. Little, and D. O'Shea. *Using Algebraic Geometry*. Number 185 in GTM. Springer, New York, 2nd edition, 2005.

[Col02] C.L. Collins. Forward kinematics of planar parallel manipulators in the Clifford algebra of P^2. *Mechanism & Machine Theory*, 37(8):799–813, 2002.

[DBKMR05] P.T. De Boer, D.P. Kroese, S. Mannor, and R.Y. Rubinstein. A tutorial on the cross-entropy method. *Annals of Operations Research*, 134(1):19–67, 2005.

[EC95] I.Z. Emiris and J.F. Canny. Efficient incremental algorithms for the sparse resultant and the mixed volume. *J. Symbolic Computation*, 20(2):117–149, 1995.

[EM99] I.Z. Emiris and B. Mourrain. Computer algebra methods for studying and computing molecular conformations. *Algorithmica, Special Issue on Algorithms for Computational Biology*, 25:372–402, 1999.

[Emi94] I.Z. Emiris, *Sparse Elimination and Applications in Kinematics*, PhD Thesis, Computer Science Division, U.C. Berkeley, 1994.

[ETV09] I.Z. Emiris, E. Tsigaridas, and A. Varvitsiotis. Algebraic methods for counting Euclidean embeddings of rigid graphs. In *Graph Drawing*, eds D. Eppstein and E.R. Gansner (Proc. Intern. Symp. Graph Drawing 2009, Chicago), LNCS, vol. 5849. Springer, pp. 195–200, 2010.

[ETV13] I.Z. Emiris, E. Tsigaridas, and A. Varvitsiotis. Mixed volume and distance geometry techniques for counting Euclidean embeddings of rigid graphs. In: A. Mucherino, C. Lavor, L. Liberti and N. Maculan, editors, *Distance Geometry: Theory, Methods and Applications*. Springer, 2013.

[FL95] J.C. Faugère and D. Lazard. The combinatorial classes of parallel manipulators combinatorial classes of parallel manipulators. *Mechanism & Machine Theory*, 30(6):765–776, 1995.

[GSR92] C.M. Gosselin, J. Sefrioui, and M.J. Richard. Solutions polynomiales au problème de la cinématique directe des manipulateurs parallèles plans à trois degrés de liberté. *Mechanism and Machine Theory*, 27(2):107–119, 1992.

[Hav98] T.F. Havel. Distance geometry: Theory, algorithms, and chemical applications. In: P. von Ragué, P. R. Schreiner, N. L. Allinger, T. Clark, J. Gasteiger, P. A. Kollman, and H. F. Schaefer III, editors, *Encyclopedia of Computational Chemistry*, pages 723–742. J. Wiley & Sons, 1998.

[Hun83] K.N. Hunt. Structural kinematics of in parallel actuated robot arms. *Trans. ASME, J. Mech. Transm. Autom. Des.*, pages 705–712, 1983.

[JRKT01] D.J. Jacobs, A.J. Rader, L.A. Kuhn, and M.F. Thorpe. Protein flexibility predictions using graph theory. *Proteins: Structure, Function, and Genetics*, 44(2):150–165, 2001.

[KGJV83] S. Kirkpatrick, C.D. Gelatt Jr, and M.P. Vecchi. Optimization by simulated annealing. *Science*, 220(4598):671, 1983.

[KPR06] D.P. Kroese, S. Porotsky, and R.Y. Rubinstein. The cross-entropy method for continuous multi-extremal optimization. *Methodology and Computing in Applied Probability*, 8(3):383–407, 2006.

[KSLO96] L.E. Kavraki, P. Svestka, J-C. Latombe, and M.H. Overmars. Probabilistic roadmaps for path planning in high-dimensional configuration spaces. *IEEE Trans. Robotics and Automation*, 12(4):566–580, 1996.

[Lam70] G. Laman. On graphs and rigidity of plane skeletal structures. *J. Engineering Mathematics*, 4:331–340, October 1970.

[Laz01] D. Lazard. Solving systems of algebraic equations. *SIGSAM Bull.*, 35(3):11–37, 2001.

[LM94] D. Lazard and J-P. Merlet. The (true) Stewart platform has 12 configurations. In *Proc. IEEE ICRA*, pp. 2160–2165, 1994.

[NA98] Y. Nourani and B. Andresen. A comparison of simulated annealing cooling strategies. *J. Physics A: Math. & General*, 31:8373, 1998.

[Rub97] R.Y. Rubinstein. Optimization of computer simulation models with rare events. *European J. Operational Research*, 99(1):89–112, 1997.

[Rub99] R.Y. Rubinstein. The cross-entropy method for combinatorial and continuous optimization. *Methodology and Computing in Applied Probability*, 1(2):127–190, 1999.

[Sch35] I.J. Schönberg. Remarks to M. Frechet's article "Sur la définition axiomatique d'une classe d'espaces vectoriels distanciés applicables vectoriellement sur l'espace de Hilbert". *Annals of Math.*, 36:724–732, 1935.

[SH87] H. Szu and R. Hartley. Fast simulated annealing. *Physics Letters A*, 122(3-4):157 – 162, 1987.

[ST10] R. Steffens and T. Theobald. Mixed volume techniques for embeddings of Laman graphs. *Comp. Geom: Theory & Appl.*, 43(2):84–93, February 2010.

[TD99] M.F. Thorpe and P.M. Duxbury, editors. *Rigidity theory and applications*. Fund. Materials Res. Ser. Kluwer, 1999.

[WH07a] D. Walter and M. Husty. On a 9-bar linkage, its possible configurations and conditions for paradoxical mobility. In *IFToMM World Congress*, Besançon, France, 2007.

[WH07b] D. Walter and M.L. Husty. A spatial 9-bar linkage, possible configurations and conditions for paradoxical mobility. In *NaCoMM*, pages 195–208, Bangalore, India, 2007.

[WT85] W. Whiteley and T.S. Tay. Generating isostatic frameworks. *Structural topology*, 11:21–69, 1985.

[Wun77] W. Wunderlich. Gefärlice annahmen der trilateration und bewegliche afchwerke i. *Zeitschrift für Angewandte Mathematik und Mechanik*, 57:297–304, 1977.

[Ver99] J. Verschelde, Algorithm 795: PHCpack: a general-purpose solver for polynomial systems by homotopy continuation, *ACM Trans. Math. Soft.*, 25(2):251–276, 1999.

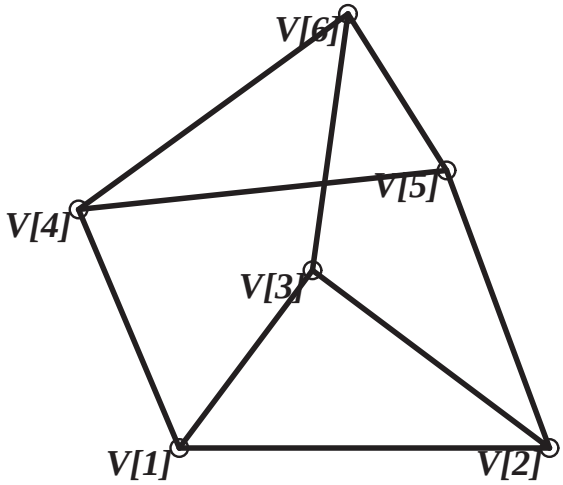

Figure 2: The Desargues linkage or, equivalently, a planar parallel robot.

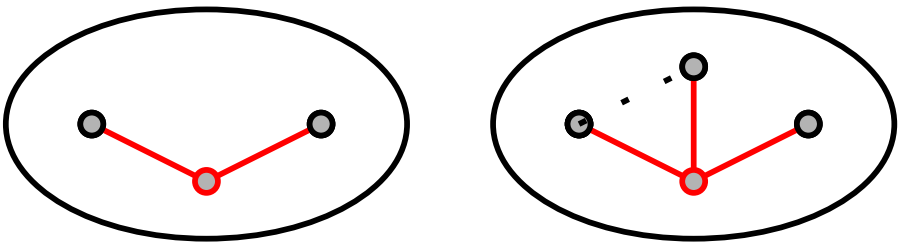

Figure 3: The planar Henneberg steps; the bottom vertex is new.

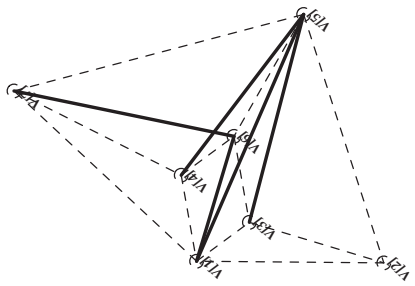

Figure 4: When the edge lengths [15], [16], [35], [45] and [67] are specified as a solution of System (2), the 11-bar linkage has only one assembly mode.

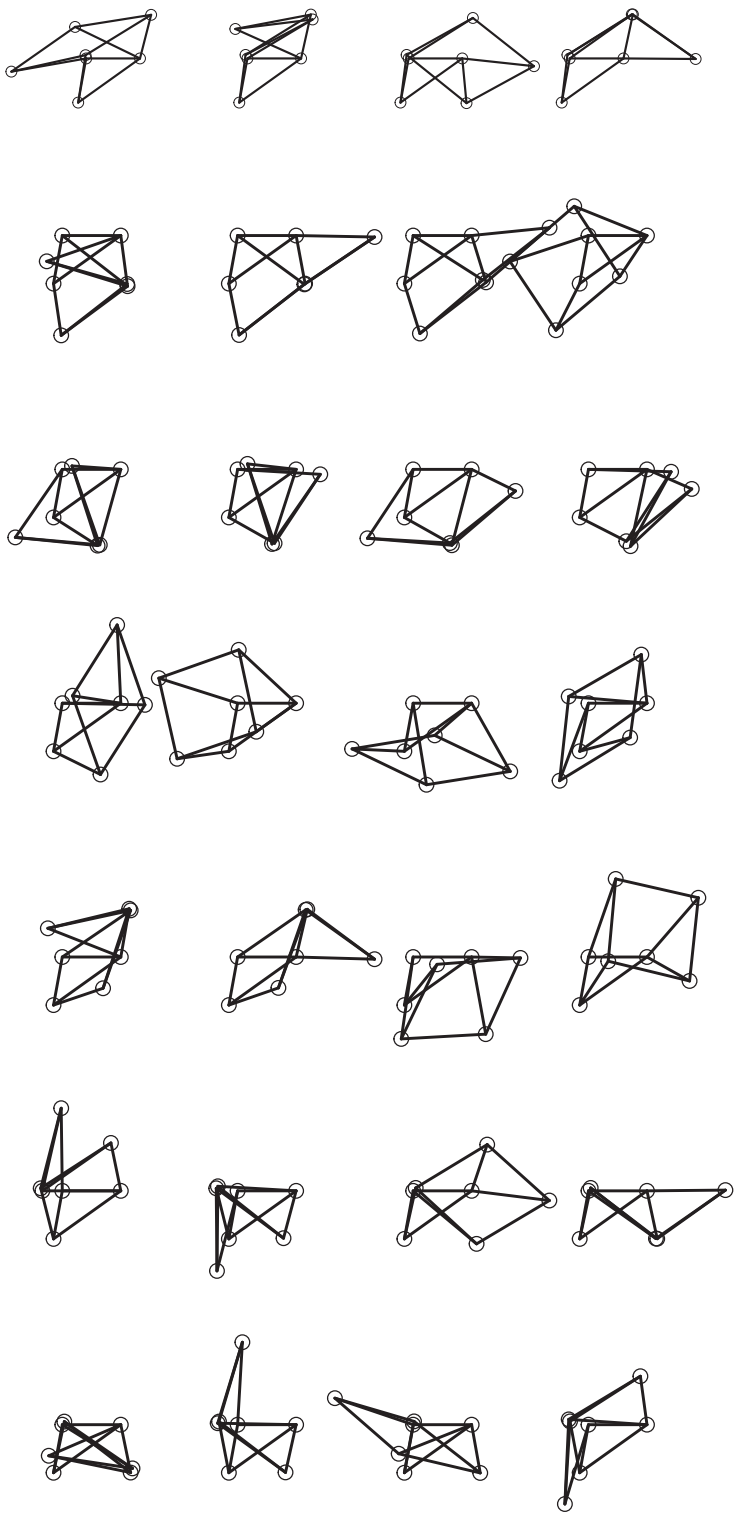

Figure 5: 28 of the 56 configurations of our linkage. The other 28 can be deduced by symmetry with respect to the horizontal axis.